Fabrication of a β-based titanium alloy for biomedical applications

Mandy Madigoe[1,2*], *Rosinah* Modiba[1], and *Lesley* Cornish[2]

[1]Advanced Materials Engineering, Council for Scientific and Industrial Research, South Africa
[2]School of Chemical and Metallurgical Engineering and DSI-NRF Centre of Excellence in Strong Materials, hosted by the University of the Witwatersrand, South Africa

Abstract. The aim of this study was to produce a titanium-based alloy with mainly β-phase and reduced Young's modulus for biomedical applications. Alloys Ti-Nb_x-Ta_5-Zr_5 (x = 20, 30, 40 at.%Nb) were prepared by arc melting then solution annealed at 950°C for 1 h, and aged at 480°C for 12 h. Optical microscopy showed mixtures of dendritic and needle-like microstructures before and after heat treatment in all alloys. X-ray diffraction (XRD) identified β-phase in all alloys. Small fractions of orthorhombic martensite (α′) and ω-phase were also detected by XRD which decreased after ageing. Alloy Ti-Nb_{20}-Ta_5-Zr_5 had the lowest Young's modulus, derived from nanoindentation hardness of 69.8 ± 7.2 GPa in the as cast condition. There was no significant change in elastic modulus of the alloy after ageing (70.8 ± 6.8 GPa). As-cast Ti-Nb_{30}-Ta_5-Zr_5 had the highest elastic modulus of 94.7 ± 3.0 GPa. The elastic modulus decreased to 84.4 ± 0.32 GPa after heat treatment.

1 Introduction

The development of titanium materials for biomedical applications is currently an area of active research world-wide and many serious attempts are made every year to improve materials properties in this field [1]. Beta-based titanium (βTi) alloys are being developed to replace the high elastic modulus commercial (alpha (α) and duplex (α + β) titanium alloys such as commercially pure Ti (CP-Ti) and Ti-6Al-4V in the biomedical sector [2]. The moduli of CP-Ti and Ti-6Al-4V lie between 100-110 GPa [5], which is significantly higher than that of human cortical bone (10-40 GPa) [3]. The high mismatch in elastic moduli of these alloys relative to the human cortical bone is caused by high amounts of α phase, which can lead to osteoporosis and poor osseointegration [4]. The βTi alloys have lower Young's modulus, high strength, superior bio-corrosion resistance and excellent biocompatibility [1, 6]. Their elastic moduli can be significantly reduced by adjusting the concentration of β stabilising elements such as Nb, Ta, Zr, Mo, etc. [7].

The β-type Ti-based alloys have been extensively developed and examples include Ti-15Mo, Ti-13Nb-13Zr, Ti-12Mo-6Zr-2Fe, Ti-35Nb-5Ta-7Zr and Ti-29Nb-13Ta-4.6Zr [8-

* Corresponding author: mseerane@csir.co.za

10]. Amongst these alloys, Ti-Nb-Ta-Zr alloys have lower Young's modulus in the range of 48 – 55 GPa, which is about 50% of that of conventional CP-Ti and Ti-6Al-4V alloys [11-13]. However, the lowest Young's modulus reported so far in bulk Ti-based alloys developed for biomedical applications is 40 GPa for the Ti-35Nb-4Sn alloy [14]. The alloying elements Nb and Ta stabilise the β phase and lowering the elastic modulus [15]. Mohammed et al. [1] reported the β phase as the largest contributor to the reduction of the Young's modulus because it has the lowest modulus, 35.29 GPa, than the other phases: α, hexagonal martensite (α′), orthorhombic martensite (α″) and omega (ω) in these Ti alloys. Niobium, acting as a β-phase stabiliser and a biocompatible element, has attracted much attention and it has been added to many β-type Ti-based alloys and near β-type Ti-based alloys [2]. Zirconium, which is a neutral element, enhances strength and improves elasticity while suppressing the precipitation of omega (ω) phase when dissolved in titanium [9, 16]. Tantalum is expected to contribute to the stabilisation of the β phase and improve mechanical performance [9]. The aim of this work was to fabricate a β Ti-Nb-Ta-Zr alloy with reduced Young's modulus by arc melting and heat treatment, targeted for biomedical applications.

2 Experimental methods

The Ti-Nb_x-Ta_5-Zr_5 (x = 20, 30, 40 at% Nb) alloys were produced by button arc melting on a water-cooled copper hearth using pure Ti, Nb, Ta and Zr metal powders as raw materials. The as-cast ingots were solution annealed under argon atmosphere at 950°C for 1 h and quenched, then aged for 12 h at 480°C followed by furnace cooling for homogenisation and precipitation hardening.

The as-cast and heat treated buttons were analysed for phases using optical microscopy (OM Leica DMI5000 M) and X-ray diffraction (EMPYREAN diffractometer system). The hardnesses and Young's moduli were measured by a Vickers micro-hardness tester (Future Tech. Corp., FM-700) and a nano-indenter (Anton Paar, TTX-NHT^3). The buttons were cut, ground and polished, then etched in a 10 vol.% HF, 10 vol.% HNO_3 + glycerol solution to reveal the microstructures. X-ray diffraction measurements were carried out at 45 kV and 40 mA using monochromatic Cu Kα radiation (λ = 0.17890 nm). Nano-indentation was done at 400 mN load at a dwell time of 20 seconds. Vicker's micro-hardness test was done at 500 gf at a dwell time of 15 seconds.

3 Results and discussion

3.1 Microstructural analysis

The microstructure of the alloys before and after heat treatment are shown in Figure 1. All the alloys had β phase in the as-cast and heat treated conditions. The β stabilising elements and treatment conditions contributed to the formation of dendritic and basket-weave microstructures [17] Figure 1a shows a dendritic structure with some acicular martensite (α′), a basket-weave structure, in the as-cast condition. According to ImageJ analysis, increasing niobium content resulted in higher volume fraction of β phase, Table 1. For 40 at.% Nb, less alpha was seen in the as-cast condition. Ageing gave regions of α phase within the main β phase for most alloys, except for Ti-Nb_{30}-Ta_5-Zr_5, which only had β-rich dendrites and some areas of acicular martensite. Nasakina et al. [18] and Elias et al. [19] obtained similar morphologies of the microstructures of alloy Ti-Nb-Ta-Zr produced by arc melting. Ageing treatment resulted in increased amount of β phase except for alloy Ti-Nb_{40}-Ta_5-Zr_5.

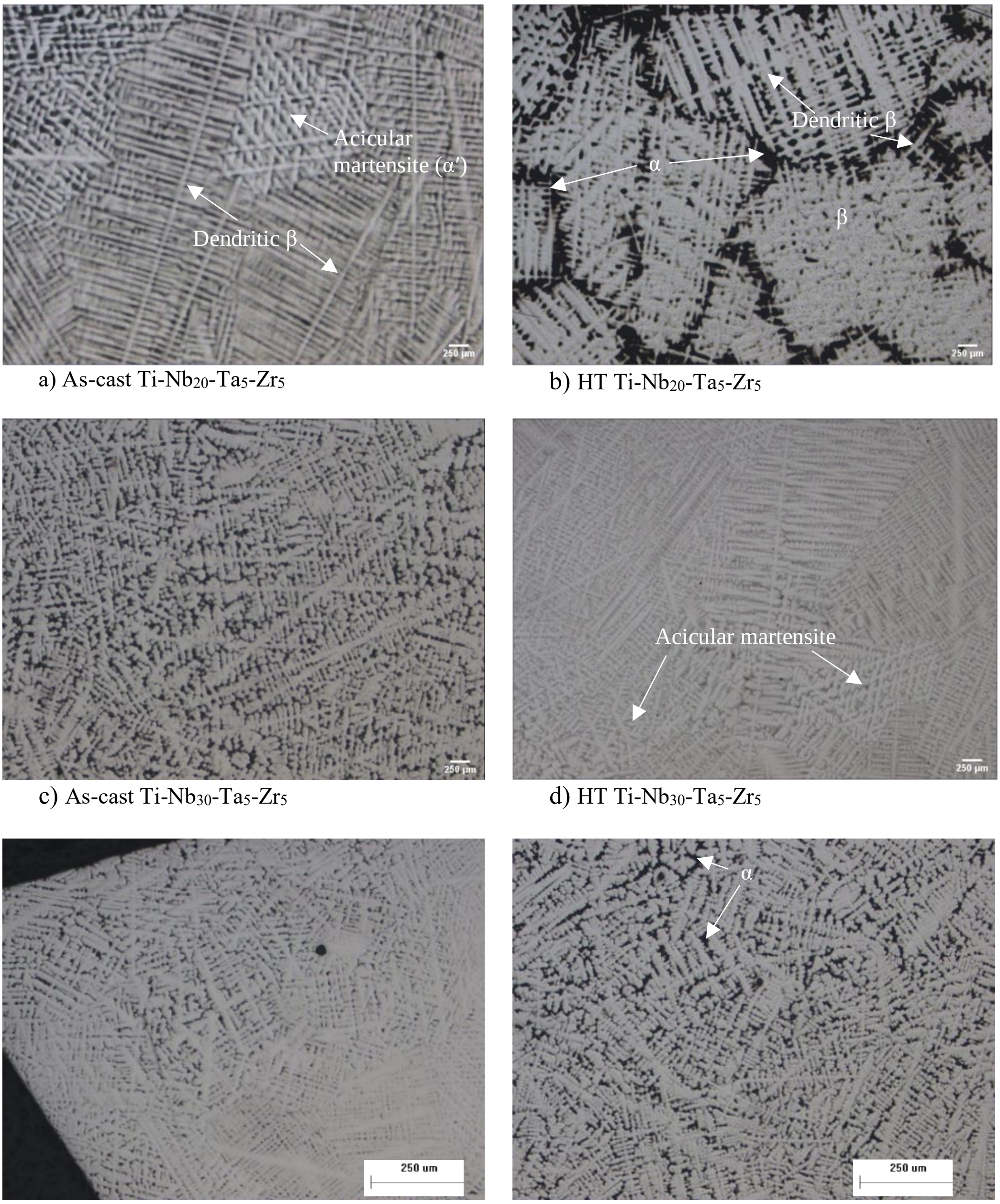

a) As-cast Ti-Nb_{20}-Ta_5-Zr_5
b) HT Ti-Nb_{20}-Ta_5-Zr_5
c) As-cast Ti-Nb_{30}-Ta_5-Zr_5
d) HT Ti-Nb_{30}-Ta_5-Zr_5
e) As-cast Ti-Nb_{40}-Ta_5-Zr_5
f) HT Ti-Nb_{40}-Ta_5-Zr_5

Fig. 1. Optical micrographs of as-cast (a, c & e) and heat treated (b, d & f) alloys Ti-Nb_{20}-Ta_5-Zr_5, Ti-Nb_{30}-Ta_5-Zr_5 and Ti-Nb_{40}-Ta_5-Zr_5.

https://doi.org/10.1051/matecconf/202237003008

Table 1. Phase fraction data of alloys Ti-Nb_{20}-Ta_5-Zr_5, Ti-Nb_{30}-Ta_5-Zr_5 and Ti-Nb_{40}-Ta_5-Zr_5

Nb content (at.%)	**As-cast phase fraction**		**Heat treated phase**	
	%α	**%β**	**%α**	**%β**
20	31.2	68.8	26.2	73.8
30	23.4	76.6	4.2	95.8
40	11.6	88.4	20.2	79.8
ImageJ analysis	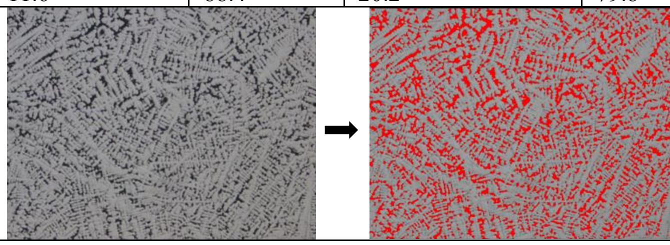			

3.2 X-ray diffraction results

Figure 2 shows the XRD patterns of the samples in the as-cast and heat treated conditions. Diffraction peaks corresponded to the β phase for all samples with small amounts of ω and α phases, which appeared to diminish after ageing. The XRD results agreed with the microstructures in Figure 1 even though α′ and ω phases were not identified in the microstructures. Larger intensity peaks of β phase were observed in Ti-Nb_{20}-Ta_5-Zr_5 after heat treatment. Small fractions of α phase were detected in aged alloys Ti-Nb_{30}-Ta_5-Zr_5 and Ti-Nb_{40}-Ta_5-Zr_5 which shows its precipitation [20], although the Ti-Nb_{30}-Ta_5-Zr_5 OM microstructure does not show the phase. As-cast alloys Ti-Nb_{20}-Ta_5-Zr_5 and Ti-Nb_{40}-Ta_5-Zr_5 had similar peaks with higher background counts in the range $42<2\theta<50^{o}$ which were indexed as hexagonal martensite (α′) and ω phase.

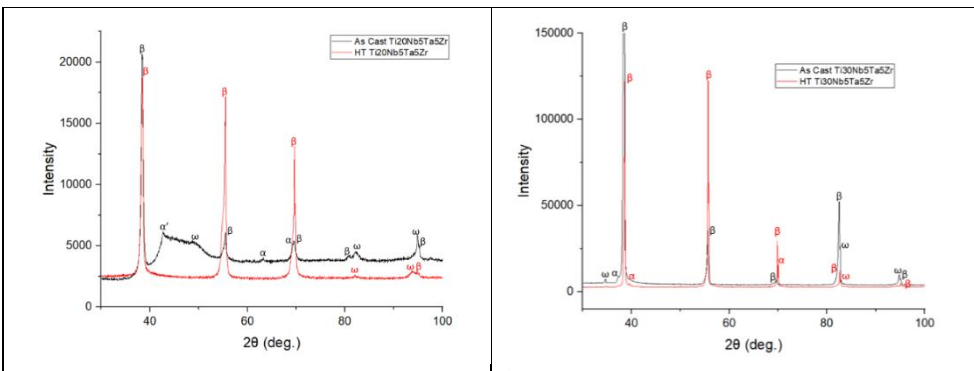

a) Ti-Nb_{20}-Ta_5-Zr_5 b) Ti-Nb_{30}-Ta_5-Zr_5

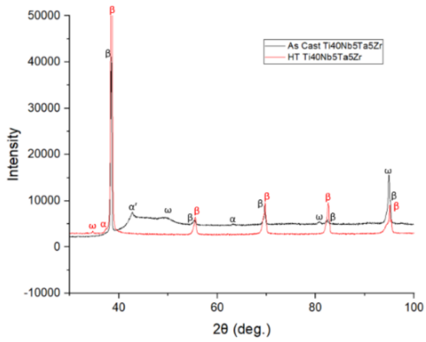

c) Ti-Nb_{40}-Ta_5-Zr_5

Fig. 2. XRD patterns of: a) Ti-Nb_{20}-Ta_5-Zr_5, b) Ti-Nb_{30}-Ta_5-Zr_5 and c) Ti-Nb_{40}-Ta_5-Zr_5 samples before and after heat treatment.

3.3 Hardness results

Figure 3 shows the Vickers micro-hardness results of the alloys. Alloy Ti-Nb_{30}-Ta_5-Zr_5 had the highest hardness of 398 ± 18.6 HV, as shown in this figure and Table 2. However, the hardness decreased to 350 ± 3.3 HV after heat treatment due to decreased α phase. Alloy Ti-Nb_{20}-Ta_5-Zr_5 had a slight increase in hardness after heat treatment and this can be attributed to the presence of α phase detected during XRD analysis.

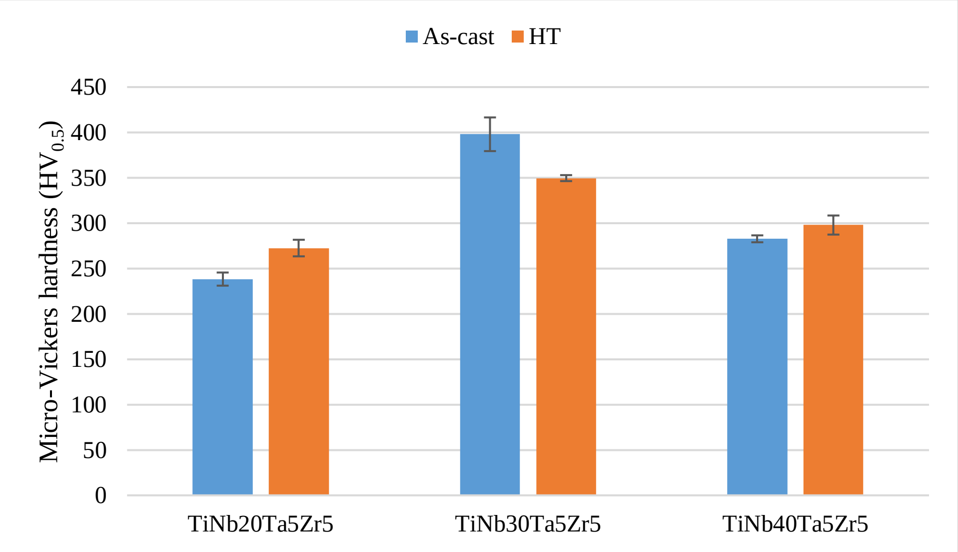

Fig. 3. Variation of hardness of the as-cast and heat treated alloys a) Ti-Nb_{20}-Ta_5-Zr_5, b) Ti-Nb_{30}-Ta_5-Zr_5 and c) Ti-Nb_{40}-Ta_5-Zr_5.

Table 2. Vickers micro-hardness of the alloys before and after heat treatment.

Alloy	Vickers micro-hardness ($HV_{0.5}$)	
	As-cast	HT
Ti-Nb_{20}-Ta_5-Zr_5	238 ± 7.2	273 ± 9.1
Ti-Nb_{30}-Ta_5-Zr_5	398 ± 18.6	350 ± 3.3
Ti-Nb_{40}-Ta_5-Zr_5	283 ± 3.8	298 ± 10.5

3.4 Nano-indentation results

Table 3 shows the Young's modulus of the alloys in their respective conditions. Alloy Ti-Nb_{20}-Ta_5-Zr_5 had the lowest Young's modulus of 69.8 ± 7.2 GPa in the as-cast condition although there was a large standard deviation. The modulus increased slightly after heat treatment, which was attributed to precipitation of α phase (Figure 1b) even though the phase was not detected by XRD, so must have been less than 4 vol.%. Alloy Ti-Nb_{30}-Ta_5-Zr_5 had the highest Young's modulus of 94.7 ± 3.0 GPa in the as-cast condition. The modulus reduced to 84.4 ± 0.3 GPa after heat treatment and this can be attributed to a decrease in α phase (Figure 1d).

Figure 4 shows nano-indentation test results for as-cast and heat treated samples, with the curves showing the elastic behaviour (E_{IT}). Heat treated Ti-Nb_{40}-Ta_5-Zr_5 alloy followed the same load-displacement recovery path as the as-cast alloy, with only 2% shift after treatment (*%shift = 100 x (new penetration depth – old penetration)/old penetration depth*). The load-displacement curve of alloy Ti-Nb_{30}-Ta_5-Zr_5 shifted to the right by 16% after heat treatment, indicating softening. A 6% shift to the left for alloy Ti-Nb_{20}-Ta_5-Zr_5 was observed after heat treatment, hence a slight increase in hardness. The nano-indentation E_{IT} for all the alloys was in agreement with Vicker's micro-hardness response.

Table 3. Elastic modulus of the alloys before and after heat treatment.

Alloy	Elastic Young's modulus (GPa)	
	As-cast	HT
Ti-Nb_{20}-Ta_5-Zr_5	69.8 ± 7.2	70.8 ± 6.8
Ti-Nb_{30}-Ta_5-Zr_5	94.7 ± 3.0	84.4 ± 0.3
Ti-Nb_{40}-Ta_5-Zr_5	80.5 ± 1.1	84.1 ± 2.5

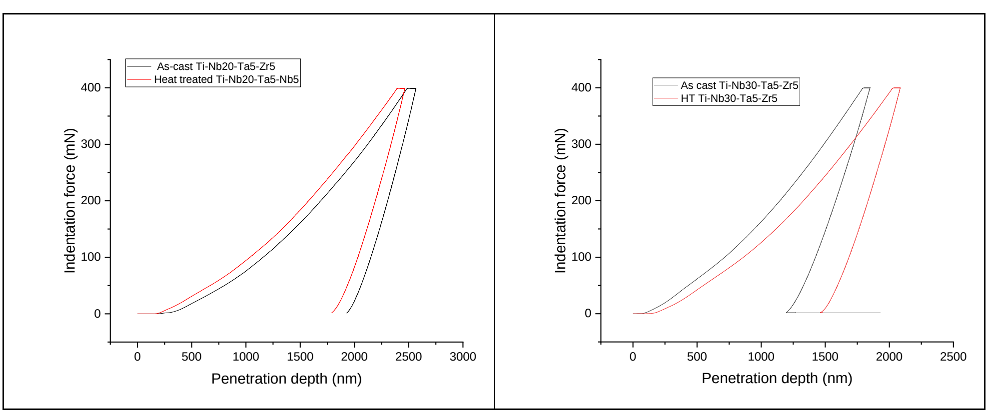

a) Ti-Nb_{20}-Ta_5-Zr_5	b) Ti-Nb_{30}-Ta_5-Zr_5

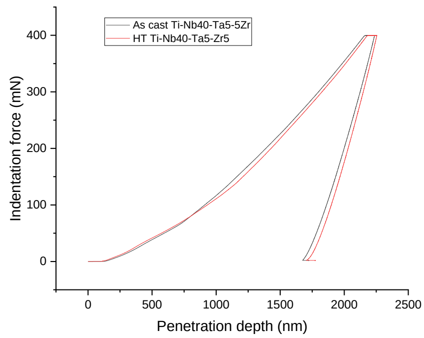

c) Ti-Nb_{40}-Ta_5-Zr_5

Fig. 4. Nano-indentation load-displacement curves of the as-cast and heat treated alloys: a) Ti-Nb_{20}-Ta_5-Zr_5, b) Ti-Nb_{30}-Ta_5-Zr_5 and c) Ti-Nb_{40}-Ta_5-Zr_5.

The alloys had mainly β dendrites with small areas of α. Secondary phases such as α′ (hexagonal), α″ (orthorhombic) and ω phase were not identified under optical microscopy. However, XRD identified the ω phase. The XRD results also showed a high background between 2θ = 42° to 50° which were indexed as α′ and ω phases. These findings require further analysis by scanning electron microscopy (SEM) and more XRD analyses. Alloy Ti-Nb_{20}-Ta_5-Zr_5 had the desired microstructure and lower Young's modulus. Ageing improved the hardness of the alloy although the precipitation of α phase was not observed.

Conclusions

- The optical microscopy results of alloys Ti-Nb_{20}-Ta_5-Zr_5, Ti-Nb_{30}-Ta_5-Zr_5 and Ti-Nb_{40}-Ta_5-Zr_5 showed dendritic microstructures with the β as the main phase. As-cast Ti-Nb_{20}-Ta_5-Zr_5 had a mixture of dendritic and acicular phases.
- Increased niobium additions resulted in less α phase, evident of β stabilisation. Ageing resulted in increased amount of β phase for alloys Ti-Nb_{20}-Ta_5-Zr_5 and Ti-Nb_{30}-Ta_5-Zr_5. Alloy Ti-Nb_{40}-Ta_5-Zr_5 undergone precipitation of α phase.
- The XRD results confirmed the major β phase in all alloys before and after heat treatment, showing the alloys were successful as β alloys. Small fractions of α, α′ and ω phases were detected in the samples by XRD and decreased after heat treatment. Alloy Ti-Nb_{20}-Ta_5-Zr_5 had lower Young's modulus (69.8 ± 7.2 - 70.8 ± 6.8 GPa), closer to that of the human cortical bone (10-40 GPa), and good hardness.
- Decrease in hardness and elastic Young's modulus for alloy Ti-Nb_{30}-Ta_5-Zr_5 was attributed to the dissolution of α phase after heat treatment even though a small amount of the phase was detected during XRD analysis. Alloy Ti-Nb_{40}-Ta_5-Zr_5 has increased hardness and Young's modulus, which was attributed to precipitation of α phase after ageing treatment.

References

1. M.T. Mohammed, Z.A. Khan, A.N. Siddiquee, Int. J. Mater. Metall. Eng. **8**, 823 (2014)
2. Y. Li, C. Yang, H. Zhao, S. Qu, X. Li, Y. Li, Materials **7**, 1711 (2014)
3. S. Nag, R. Banerjee, J. Stechschulte, H.L. Fraser, J. Mater. Sci.: Mater. Med. **16**, 681 (2005)
4. B. Gasser, *Design and Engineering Criteria for Titanium Devices.* in Titanium in Medicine, Springer, 674 (2001)
5. C.H. Park, J.W. Park, J.T. Yeom, Y.S. Chun, C.S. Lee, Mater. Sci. Eng. A **527**, 4915 (2010)
6. L. Wang, Z. Lin, X. Wang, Q. Shi, W. Yin, D. Zhang, Z. Liu, W. Lu, Mater. Trans. **55**, 141 (2014)
7. M. Niinomi, Metall. Mater. Tran., 33A, pp 477-486 (2002)
8. D. Kuroda, H. Kawasaki, A. Yamamoto, S. Hiromoto, T. Hanawa, Mater. Sci. Eng. C **25**, 312 (2005)
9. S. Nag, R. Banerjee, H.L. Fraser, Mater. Sci. Eng. C **25**, 357 (2005)
10. M. Niinomi, T. Akahori, S. Katsura, K. Yamauchi, M. Ogawa, Mater. Sci. Eng. C **27**, 154 (2007)
11. K. Wang, Mater. Sci. Eng. A **213**, 134 (1996)
12. J.I. Qazi, H.J. Rack, Adv. Eng. Mater. **7**, 993 (2005)
13. V. Brailovskai, S. Prokoshkin, M. Gauthier, K. Inaekyan, S. Dubinskiy, M. Petrzhik, M. Filonov, Mater. Sci. Eng. C **13**, 643 (2011)
14. H. Matsumoto, S. Watanabe, S. Hanada, *Strengthening of low Young's modulus beta Ti-Nb-Sn alloys by thermomechanical processing*, in Proceedings of the Materials and Processes for Medical Devices Conference, 14-16 November 2006, Boston, MA, USA (2006)
15. L.-C. Zhang, L.-Y. Chen, Adv. Eng. Mater. **21**, 6 (2019)
16. T.Y. Zhen, Z. Lian, Mater. Sci. Eng. A **438-440**, 391 (2006)
17. R. Pederson, *Microstructure and Phase Transformation of Ti-6Al-4V*, PhD Thesis, Lulea University of Technology, 10 (2002)
18. E.O Nasakina, S.V. Konushkin, M.I. Baskakova, I.M. Fedyuk, K.V. Sergienko, A.S. Baikin, M.A. Kaplan, M.A. Sevostyanov, A.G. Kolmakov, J. Material Sci. Eng. **7**, 3-4 (2018)
19. L.M. Elias, S.G. Schneider, S. Schneider, H.M. Silva, F. Malvisi, Mater. Sci. Eng. A **432**, 109-110 (2006)
20. R.S. Sudhagara, V. Jithin, M. Geetha, R.M. Nageswara, *Heat Treatment of Metastable Beta Titanium Alloys*, in Welding – Modern Topics IntechOpen, 4 (2020)